Mathematical Geology, Vol. 38, No. 5, July 2006 (© 2006)
DOI: 10.1007/s11004-006-9038-8

Qualitative and Quantitative Characteristics of Modeled and Natural Oscillatory Zoning Patterns in Calcite[1]

N. A. Bryksina,[2,3,4] N. M. Halden,[2] and S. Mejia[2]

Four types of oscillatory zoning patterns (OZP) produced by a dynamic model are described qualitatively and quantitatively and displayed as simulated cathodoluminescence images. The behavior of the dynamic model was investigated in terms of the parameter θ, which is the ratio of diffusivities of Ca^{2+} and H_2CO_3, and in terms of the parameter γ, which is the product of θ and the ratio of concentrations of Ca^{2+} and H_2CO_3 far away from the crystal surface. Qualitatively, the dynamics of the model has been characterized by a stable focus, an unstable focus changing to a stable node or to a stable limit cycle, and by periodical behavior with constant amplitude. Quantitative characteristics, including amplitude of oscillations and duration of oscillations, change between the patterns. It is shown that the process of forming oscillatory zoning in calcite with conditions corresponding to periodical behavior with constant amplitude is very slow in comparison to other OZPs. The oscillatory zoning pattern in a natural calcite crystal is described qualitatively in terms of four general OZPs produced by the dynamic model.

KEY WORDS: dynamic model; limit cycle; stable and unstable focus; cathodoluminescence; trace element.

INTRODUCTION

Oscillatory zoning patterns (OZP) are most commonly interpreted as reflecting temporal changes in properties of the bulk fluid from which crystallization occurs (Yardley and others, 1991; Jamtveit, Wogelius, and Fraser, 1993; Bryxina and others, 2000a). Oscillatory zoning may result from the response to systematic or random variations in the external parameters controlling the growth environment (Jamtveit, 1991; Holten, Jamtveit, and Meakin, 2000; Katsev and

[1] Received 24 November 2004; accepted 17 January 2006; Published online: 8 December 2006.
[2] Department of Geological Sciences, University of Manitoba, Winnipeg, MB R3T 2N2, Canada; e-mail: bryxinan@cc.umanitoba.ca
[3] Institute of Mineralogy and Petrography, Novosibirsk 630090, Russia.
[4] 405-81 University Crescent, Winnipeg, MB R3T 4W9, Canada; e-mail: Natalia.Bryksina@nrc-cnrc.gc.ca

L'Heureux, 2000). However, other mechanisms are possible. It is known that spatio-temporal pattern can arise by self-organization. Self-organization is the spontaneous patterning of a system through its own internal dynamics (Nicolis and Prigogine, 1977; Merino, 1984; Ortoleva and others, 1987). There is many examples where self-organized oscillatory zoning has been interpreted to have occurred during crystal growth (Shore and Fowler, 1996). The best known example of a mineral commonly exhibiting oscillatory zoning is plagioclase feldspar, a solid solution series between the end-members anorthite and albite (Pearce and Kolisnik, 1990). Oscillatory zoning may also result from variations of trace elements in minerals, for example Mn in calcite. Observations of oscillatory zoning in solution-grown calcite crystals are reported by Reeder, Fagioli, and Meyers (1990). In these calcites periodic zonal variations in Mn^{2+} content observed by cathodoluminescence microscopy were not correlated with changes in any bulk solution parameters, and it was interpreted that the oscillatory behavior developed autonomously.

Natural zoning patterns in minerals often look complicated. Minerals show zones of variable width and the zones may have differing concentrations of elements as well as differing optical characteristics (Halden, 1996; L'Heureux and Fowler, 1996; Fowler and L'Heureux, 1996; Bryxina and others, 2000b, 2001a; Bryxina, Halden, and Ripinen, 2002). Optically zones may appear to be more intense while other zones might dwindle to the point they disappear, some zones may appear sharply defined while others are diffuse, also minerals might show what look like continuously changing zoning patterns. A study of OZP includes not only the examination of natural occurrences and experimental synthesis, but also physicochemical modeling (Haase and others, 1980; Allegre, Provost, and Jaupart, 1981; Wang and Merino, 1990, 1992, 1993, 1995; L'Heureux and Fowler, 1996; Jamtveit 1991; Wang and Wu, 1995; Merino and Wang, 2001; L'Heureux and Jamtveit, 2002).

Wang and Merino (1992) describe a dynamic model for calcite grown from an aqueous solution containing growth-inhibiting cations such as Mn^{2+}. This model, based on a feedback involving H^+ accumulation, surface adsorption, repulsion of inhibiting Mn^{2+} ions, calcite growth acceleration and faster generation of H^+ ions (which closes the cycle) is able to autonomously produce oscillatory changes of Ca^{2+} and H_2CO_3 concentrations adjacent to a calcite growth surface without large-scale changes in bulk water chemistry. The linear stability analysis of this model is made by Wang and Merino (1992), and the periodical solutions have been found for specific parameter values. The complete qualitative analysis by taking into account non-linear terms of the model was made by Bryxina and Sheplev (1997, 2001b), and all possible phase portraits were found: four in the parameter value's region of unique equilibrium, and 47 in the region of multiplicity. While 51 phase portraits can be produced by the equations, a real physical system may be

represented by fewer portraits, these being limited by the magnitude of the natural parameters involved.

Here we present four examples from the 51 possible phase portraits which capture, in a general way, the appearance of oscillatory zoning patterns. Each example corresponds to specific parameter values of the model. We describe qualitatively and quantitatively four general types of OZP and establish in a "petrographic" sense what such patterns might look like. Then we investigate the behavior of the model in terms of these four OZPs depending on the parameter θ, which is the ratio of diffusivities of Ca^{2+} and H_2CO_3. We also investigate the behavior of the model depending on the parameter γ, which is the product of θ and the ratio of concentrations of Ca^{2+} and H_2CO_3 far away from the crystal surface. And last we present a natural oscillatory zoning pattern in calcite crystal from the Rossland area (BC, Canada) and characterize it qualitatively in terms of four modeled OZPs.

DYNAMIC MODEL FOR CALCITE CRYSTALLIZATION

Wang and Merino (1992) provide both a physicochemical model as well as a physical sense of the parameters they used, including diffusion rates and species concentrations for oscillatory calcite growth. After a series of simplifying assumptions this model can be reduced to the following two-dimensional model with five parameters ($\theta, \lambda, \beta_1, \beta_2, \gamma$):

$$\begin{aligned} \frac{du}{dt} &= 1 - u - \lambda(1 + \beta_1 v + \beta_2 v^2)u \\ \frac{dv}{dt} &= -v + \gamma\lambda(1 + \beta_1 v + \beta_2 v^2)u, \end{aligned} \tag{1}$$

where u and v are scaled concentrations of Ca^{2+} and H_2CO_3, respectively, next to the crystal surface; all quantities are dimensionless. Wang and Merino (1992) evaluated the magnitude of the parameters involved in the model (Eq. (1)) and deduced the following approximate parameter ranges within which calcite can incorporate oscillatory concentrations of trace elements: $\lambda > 0.0065$, $\gamma > 1.4$, $\beta_1 > 18$, $\beta_2 > 8$ and $\theta < 1$.

Using these results and a computer package MATHEMATICA we integrate the model (Eq. (1)) numerically and calculate the concentrations of Ca^{2+} (u) and H_2CO_3 (v) with respect to time. According to the assumptions made by Wang and Merino (1992) the amount of a trace element (such as Mn^{2+}) incorporated into calcite is proportional to the amount of a trace element adsorbed on the growth surface and depends on pH at the growth front. The oscillatory pH leads

to an oscillatory variation of trace elements (including Mn^{2+}) in calcite crystals. We calculate the H^+ content at the crystal surface using (Eq. (18)) from the paper (Wang and Merino, 1992, p. 590) together with H_2CO_3 concentrations (v) obtained from the model (Eq. (1)). As the Mn^{2+} content is inversely proportional to the H^+ content, the next step is to construct a synthetic image to simulate cathodoluminescence. Here the Mn^{2+} concentrations are fitted to a 255 gray level scale and assigned colors from black to the yellow orange region of the spectrum where yellow is assigned the highest values, orange intermediate values and black the lowest values. The zoning is then reproduced as a 2 dimensional synthetic image. Output of Mn^{2+}concentrations ($c_{Mn^{2+}}$) from MATHEMATICA are normalized to a 255 color scale using:

$$\frac{c_{Mn^{2+}} \times 255}{\max},$$

where max was the maximum value of Mn^{2+} concentrations, this scale provides for a visual representation and comparison of the OZP. When the amplitude of oscillations is small, the scale for Mn^{2+} concentrations can be stretched using

$$\frac{(c_{Mn^{2+}} - \min) \times 255}{\max - \min},$$

where min was the minimum value of Mn^{2+} concentrations.

DYNAMIC BEHAVIOR AND ZONING CHARACTERISTICS OF FOUR MAIN OZP

Numerical solving of the model (Eq. (1)) requires parameter values (Table 1) and a description of the initial conditions for variables u and v. In choosing the initial conditions, it is very important to know the number, type and stability of the equilibrium solutions. Taking initial values close to the coordinates of equilibrium gives the solution which is defined by the behavior of the dynamic model near this equilibrium. On the other hand, taking initial values relatively far away from the coordinates of equilibrium may result in missing some solutions of the model, because of the multiplicity of the equilibrium solutions. In this case, the qualitative analysis (Bryxina and Sheplev, 1997, 2001b) is very helpful, because it gives a clear view of the behavior of the dynamic model near all equilibrium solutions.

Table 1. Parameter Values Used to Generate OZP

Type of OZP	θ	λ	β_1	β_2	γ
OZP I	0.07	0.01	70	100	2
OZP II	0.2	0.01	60	80	2
OZP III	0.25	0.01	30	80	2
OZP IV	0.3495	0.0108	40	100	1.5093

OZP I

When the parameter θ changes over a very limited range: 0.07–0.11 and the remaining parameters are kept constant ($\lambda = 0.01$, $\beta_1 = 70$, $\beta_2 = 100$, $\gamma = 2$), the scaled concentrations of Ca^{2+} (column A, Fig. 1) show asymmetric profiles with a gradual sloping increase followed by a sharp decline. Sharp spikes in the scaled concentrations of H_2CO_3 (column B, Fig. 1) correspond to the sudden drops in Ca^{2+} concentrations. The relation of Ca^{2+} concentrations to H_2CO_3 concentrations is shown by the plots in column C of Figure 1. These plots show the behavior of the model (Eq. (1)) on the phase plane $\{Ca^{2+}, H_2CO_3\}$. Here are the phase trajectories, which began at the point $\{0.22; 1.56\}$, move away from it, and then go to a closed trajectory called a limit cycle (LC). The starting point is the coordinates of the equilibrium (which is unique for the parameter values used in this example), because we wish to illustrate the behavior of the model near equilibrium. For example, taking the initial conditions relatively far away from the coordinates of the equilibrium, such as $\{0.5; 1.5\}$, will give the phase trajectory moving from this starting point directly to a limit cycle without a region of oscillations with increasing amplitude (OIA). The behavior of a dynamic model near equilibrium is characterized by the signs of determinant (Δ) and the trace (σ) of Jacobian matrix of linearized dynamic model (Andronov and others, 1967; Bryxina and Sheplev, 1997, 2001b). Calculating Δ and σ for all three cases presented in Figure 1 gives: $\Delta > 0$, $(\sigma/2)^2 - \Delta < 0$, $\sigma > 0$. Therefore, in this case, the equilibrium is characterized as an unstable focus (UF). In terms of describing the dynamics of the system, an unstable focus is where the tendency of the system is to diverge in time with oscillations of increasing amplitude (OIA), and the phase portrait is essentially a divergent spiral until it reaches a LC. That is what we see in column C of Figure 1.

Column D in Figure 1 shows a graphic representation of the zoning patterns. From a "petrographic" perspective, if these were views of a crystal, the growth history would be from left to right and the pattern would be described as an oscillatory zoning pattern. The zones would be described as showing an asymmetric gradational change in color from yellow to orange followed by a sharp boundary. The synthetic OZPs (Fig. 1(D)) are all very similar to each other showing only small changes in the onset of oscillations with constant amplitude (OCA) after a

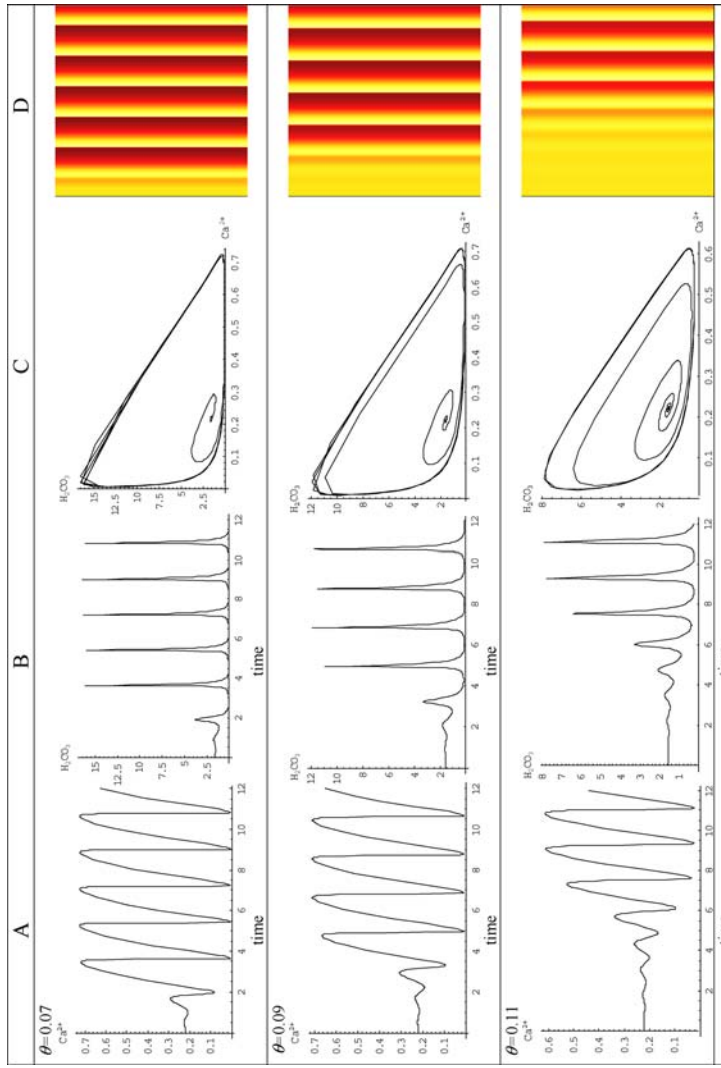

Figure 1. Behavior of the model (Eq. (1)) when the values of parameter θ vary from 0.07 to 0.11, and all other parameters are fixed: $\lambda = 0.01$, $\beta_1 = 70$, $\beta_2 = 100$, $\gamma = 2$. Starting point: $u = 0.22$, $v = 1.56$. Quantitative characteristics of OZP I at $\theta = 0.07$: time = 2, ALC: $|u| = 0.7$, $|v| = 15$. (A) Scaled concentrations of Ca^{2+} (u) depending on dimensionless time (time). (B) Scaled concentrations of H_2CO_3 (v) depending on dimensionless time (time). (C) Phase portraits of the model. (D) OZP generated by the model.

region of oscillations of increasing amplitude (OIA). Also, there are small changes in the intensity of the color (Fig. 1(D)). With increasing θ the onset of OCA becomes later and the color intensity declines slightly. The pattern is characterized by a time of OIA, and the amplitude of a limit cycle (ALC) described by $|u|$—amplitude of oscillations of Ca^{2+} concentration and $|v|$—amplitude of oscillations of H_2CO_3 concentration; these may be used to quantitatively characterize OZP I. For $\theta = 0.07$, the quantitative characteristics are: time $= 2$, $|u| = 0.7$, $|v| = 15$. As θ increases, the duration of the OIA increases, but the amplitude of the LC decreases.

OZP II

At the parameter values for OZP II (Table 1) there is also one equilibrium solution of the model (Eq. (1)). Qualitative analysis gives $\Delta > 0, (\sigma/2)^2 - \Delta < 0$, $\sigma < 0$, that is, the equilibrium is a stable focus (SF). In this case, the model produces oscillations with decreasing amplitude (ODA) for Ca^{2+} concentrations (Fig. 2(A)) and for H_2CO_3 concentrations (Fig. 2(B)). The visible ODA for Ca^{2+} concentration go until time $= 35$. This quantity may be used as a quantitative characteristic for OZP II. The phase trajectory corresponding to these oscillations is a convergent trajectory in the phase plane (Fig. 2(C)), which goes from the starting point $\{0.5;\ 1.5\}$ to the equilibrium with the coordinates $\{0.29;\ 1.43\}$. The two-dimensional pattern (Fig. 2(D)) shows symmetrical gradational zones of color that decrease in intensity. OZP II evolves to a stable focus irrespective of the starting point for the model in terms of the concentrations of Ca^{2+} and H_2CO_3.

OZP III

In contrast to OZP I and OZP II, three equilibrium solutions can be generated by the model (Eq. (1)) using the parameter values for OZP III (Table 1). In this case, depending on the initial conditions the model may evolve to one or another equilibrium solution separated on the phase plane by what is known as a saddle which is itself equilibrium (Andronov and others, 1967). Location of a saddle and another two equilibrium solutions (State 1 and State 2) on the phase plane $\{Ca^{2+}; H_2CO_3\}$ are shown in Figure 3(C). For State 1, and the region around State 1, concentrations of Ca^{2+} are low ($u = 0.39$) and the model will evolve from what is an unstable focus (UF). State 2 has the highest Ca^{2+} concentration ($u = 0.97$) and the model will evolve to a stable node (SN), which attracts the system. The third equilibrium solution (a saddle) exists between State 1 and State 2 at intermediate Ca^{2+} concentrations but does not produce oscillatory zoning. Note, even though there is an UF characterizing State 1, there is no limit cycle, in this case, the system is attracted to another equilibrium, which distinguishes this pattern from

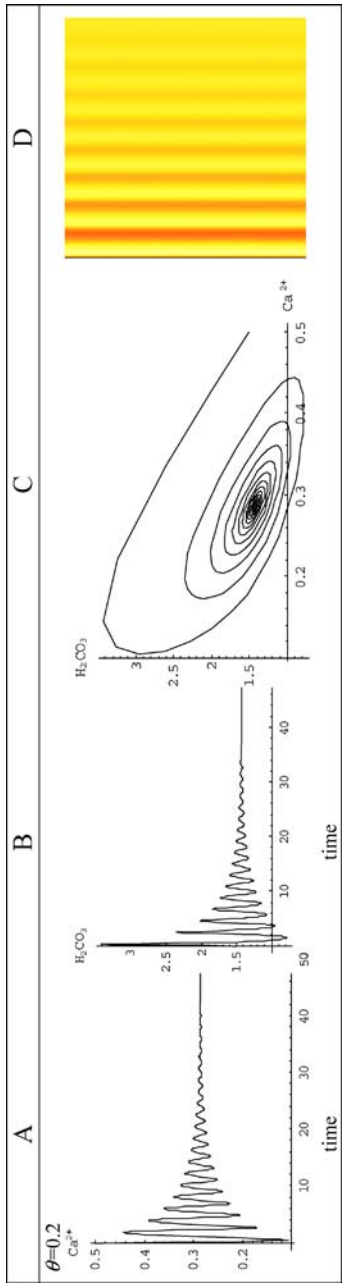

Figure 2. Behavior of the model (Eq. (1)) at the parameter values: $\theta = 0.2, \lambda = 0.01, \beta_1 = 60, \beta_2 = 80, \gamma = 2$. Starting point: $u = 0.5$, $v = 1.5$. Quantitative characteristics of OZP II: time=35. (A) Scaled concentrations of Ca^{2+} (u) depending on dimensionless time (time). (B) Scaled concentrations of H_2CO_3 (v) depending on dimensionless time (time). (C) Phase portraits of the model. (D) OZP generated by the model.

OZP I. If we take the starting point $\{0.4; 1.2\}$ close to State 1, then the system evolves away from State 1 in an oscillatory fashion as OIA and is finally drawn gradually towards a constant value (State 2). On the other hand, if the starting point is chosen somewhat farther from State 1, for example at point $\{0.45; 1.3\}$ on phase plane $\{Ca^{2+}; H_2CO_3\}$, then the system moves from the starting point to the constant value (SN) without oscillations, which means there will be no zones. There is a region of starting points around State 1 which will produce OIA, outside this region the system will be right away attracted to a constant value.

Figures 3(A) and (B) show oscillations with increasing amplitude (OIA) depending on time for scale concentrations of Ca^{2+} and H_2CO_3 respectively. OIA go until time = 15. This quantity is taken as a quantitative characteristic of OZP III. Zoning produced by the model in this case is characterized by increasing color intensity changing finally to a zone of homogenous color (Fig. 3(D)).

OZP IV

Figure 4 shows oscillatory zoning produced by the model (Eq. (1)) at the bifurcation parameter values (OZP IV, Table 1). Bifurcation values of the parameters are some critical values, which when changed can cause qualitative differences in the behavior of a dynamic model. To find these values we use the results of the qualitative analysis of the model (Eq. (1)) obtained by Bryxina and Sheplev (1997, 2001b), and calculated by them Lyapounov coefficients L_1, L_2 and L_3. It is shown (Bryxina and Sheplev, 1997, 2001b) that L_1 and L_2 may have positive or negative values, but L_3 is negative in the whole domain of parameters in which $\sigma = 0$, $L_1 = 0$ and $L_2 = 0$. Also, they showed that the number of parameters of the model (Eq. (1)) can be reduced to four by the following substitution:

$$x = 1 - u \quad y = \beta_1 v \quad B = \beta_1 \gamma / \theta \quad g = 1/\beta_1 \gamma \quad \beta = \beta_2 / \beta_1^2 \qquad (2)$$

Bifurcation values of the parameters are found from the conditions: $\sigma = 0, L_1 = 0$, $L_2 = 0$. The expressions for σ, L_1, L_2 depending on the parameters of the model can be found in Bryxina and Sheplev (1997, 2001b). As we have four parameters (λ, B, g, β) and only three equations, one parameter must be fixed, for example $\beta = 0.0625$. This value of the parameter β is obtained from (Eq. (2)), when we take $\beta_1 = 40$ and $\beta_2 = 100$, at which three equilibrium solutions can be generated by the model. From the conditions $L_1 = 0$ and $L_2 = 0$ we find $\lambda = 0.0108$ and $g = 0.017$, and from the condition $\sigma = 0$ we find the value of the parameter $B = 172.75$. Using (Eq. (2)) we can return to the primary parameters remembering that there is an option to choose one parameter. So, taking $\beta_1 = 40$ and $\beta_2 = 100$ we calculate $\theta = 0.3495$ and $\gamma = 1.5093$.

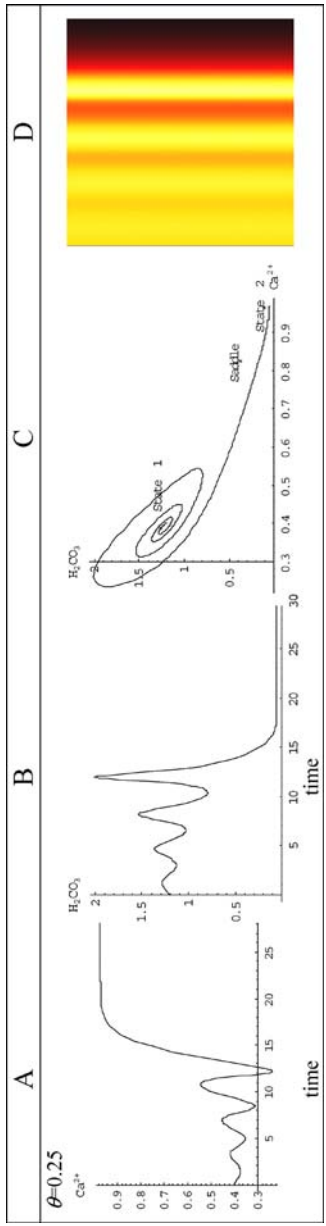

Figure 3. Behavior of the model (Eq. (1)) at the parameter values: $\theta = 0.25$, $\lambda = 0.01$, $\beta_1 = 30$, $\beta_2 = 80$, $\gamma = 2$. Starting point: $u = 0.4$, $v = 1.2$. Quantitative characteristics of OZP III: time = 15. (A) Scaled concentrations of Ca^{2+} (u) depending on dimensionless time (time). (B) Scaled concentrations of H_2CO_3 (v) depending on dimensionless time (time). (C) Phase portraits of the model. (D) OZP generated by the model.

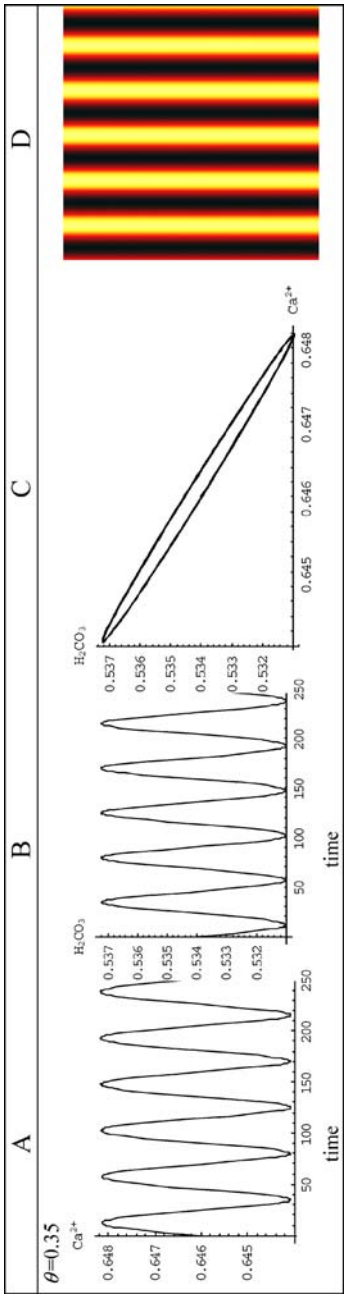

Figure 4. Behavior of the model (Eq. (1)) at the parameter values: $\theta = 0.3495$, $\lambda = 0.0108$, $\beta_1 = 40$, $\beta_2 = 100$, $\gamma = 1.5093$. Starting point: $u = 0.646$, $v = 0.534$. Quantitative characteristics of OZP IV: AOCA: $|u| = 0.004$, $|v| = 0.006$. (A) Scaled concentrations of Ca^{2+} (u) depending on dimensionless time (time). (B) Scaled concentrations of H_2CO_3 (v) depending on time. (C) Phase portraits of the model. (D) OZP generated by the model.

There are three equilibrium solutions of the model (Eq. (1)) at the bifurcation parameter values (OZP IV, Table 1): a center (CE), a saddle and a stable node (SN). Using initial values close to the center, such as $\{0.646; 0.534\}$, gives periodic solutions, which are symmetrical around the coordinates of the center (Figs. 4(A) and (B)). In this case, the phase trajectory is a closed line (Fig. 4(C)). Taking initial values relatively far away from the coordinates of the center results in convergence to the equilibrium solution with the highest Ca^{2+} concentration ($u = 0.964$) which is a stable node (no oscillations). Figure 4(D) shows the OZP produced at the bifurcation values of the parameters, where zones in terms of color are symmetrical and change from light to dark. However, the amplitude of the oscillations is very small in comparison to the other patterns. In this case, in order to make the OZP IV pattern more visible, we stretched the scale as described early. As the quantitative characteristic for OZP IV we can use the amplitude of oscillations:$|u| = 0.004$, $|v| = 0.006$.

Comparison of OZP

As the model (Eq. (1)) gives us the variations in Ca^{2+} content depending on time, we can compare the times, which are needed for forming different OZPs. Figure 1 (columns A and B, the first row) shows that when the process of forming oscillatory zoning in calcite corresponds to the regime described by OZP I, the dimensionless time of one period of the limit cycle is approximately equal to 2. From Figure 2 we can see that the dimensionless time of one period of oscillations with decreasing amplitude (OZP II) is approximately equal to 3. The dimensionless time of one period of oscillations with increasing amplitude (OZP III) is approximately equal to 8.5 (Fig. 3). The dimensionless time of one period in OZP IV is approximately equal to 45 (Fig. 4). This means that OZP IV would form very slowly in comparison to other OZPs. The fastest process for forming of oscillatory zoning corresponds to the conditions required to form OZP I.

EFFECT OF DIFFUSIVITY

It might be anticipated that in natural systems we could expect a wide range of starting concentrations for ions of interest and variations in diffusivity that could be affected by temperature and bulk geochemistry. According to Li and Gregory (1974), the diffusivity of Ca^{2+} can increase from 3.73×10^{-6} to 7.93×10^{-6} when temperature is changed from 0 to 25°C. We might expect the system to respond to changes in temperature and or concentrations making the broader system much more complex. However, in an attempt isolate some of the potential differences created by these variables, first of all, we have used fixed parameters

for equilibrium solution and allowed the diffusivity to vary over a wide range. We call this analysis as "effect of diffusivity", and the "effect of concentrations" is described in the next section.

As the parameter θ does not enter into the right hand side of (Eq. (1)), the number and the coordinates of the equilibrium solutions do not depend on θ, but as it will be shown later their type and stability depend on θ very strongly. The range predicted by Wang and Merino (1992) for θ ($\theta < 1$) is reasonable because the diffusivity for aqueous Ca^{2+} is indeed less than that for H_2CO_3 (Li and Gregory, 1974). We consider two examples, in which the parameter θ varies from 0.1 to 0.6, and two sets of other parameters are used. The first set corresponds to the case when the model has a unique equilibrium, and the second one corresponds to the case when the model has three equilibrium solutions.

Table 2 shows the changing of behavior of the model (Eq. (1)) in the first example. All parameters (except θ) correspond to OZP II (Table 1) and are fixed; the initial conditions close to the equilibrium, which is unique in this case. When θ is in the range from 0.1 to 0.17, the behavior of the model is an unstable focus and is similar to that shown in Figure 1; as θ increases, the time taken for oscillations with increasing amplitude (OIA) to change to limit cycle (LC) increases and the amplitude of limit cycle (ALC) decreases. This persists until θ is equal to 0.1855; here the type of equilibrium changes to a center with the amplitude of oscillations, such as $|u| = 0.016$, $|v| = 0.053$ and the behavior of the model becomes similar to that shown in Figure 4. Further increasing θ results in another change in type of equilibrium to a stable focus preceded by ODA, similar to that shown in Figure 2. Oscillations are visible when $\theta < 0.2$; as θ exceeds 0.2 visible oscillations eventually disappear. The time of disappearance becomes earlier as θ becomes bigger. When θ is 0.5 and higher, the model (Eq. (1)) does not produce oscillatory zoning.

Table 3 shows the results of our investigation in the case when the model (Eq. (1)) has three equilibrium solutions. Again we change only θ, and all other parameters are fixed and have the values from OZP III (Table 1). As it was mentioned above, the equilibrium solution with intermediate Ca^{2+} concentrations is a saddle. Using the results of qualitative analysis (Bryxina and Sheplev, 1997, 2001b) we calculate Δ and σ for equilibrium state with the highest Ca^{2+} concentrations (ES 2) and obtain a stable node. The equilibrium state with the lowest Ca^{2+} concentrations (ES 1) may change its type as θ changes. Table 3 shows such changes, when the initial conditions are chosen in the local region surrounding ES 1, such as $\{0.39; 1.22\}$. In Table 3, when θ changes from 0.1 to 0.27, the behavior of the model (Eq. (1)) is similar to that shown in Figure 3. As θ increases, the time taken for OIA to change to ES 2 increases. When θ is equal to 0.2934, the type of equilibrium changes to a center with the amplitude of oscillations, such as $|u| = 0.027$, $|v| = 0.01$, similar to that shown in Figure 4. Further increasing in θ results in another change in the type of equilibrium state becoming a stable focus

Table 2. Changes in Character of Zoning and Type of Equilibrium State Using Different Values of θ

θ	σ	Type of ES	Pattern development	Type of OZP	Quantitative characteristics	Figure for comparison
0.1	0.86	UF	OIA to LC	OZP I	OIA go until time = 2; ALC: $\|u\| = 0.8$, $\|v\| = 11.6$	Fig. 1
0.15	0.24	UF	OIA to LC	OZP I	OIA go until time = 10; ALC: $\|u\| = 0.58$, $\|v\| = 4.8$	Fig. 1
0.17	0.091	UF	OIA to LC	OZP I	OIA go until time = 26; ALC: $\|u\| = 0.4$, $\|v\| = 2.6$	Fig. 1
0.1855	0	CE	OCA	OZP IV	AOCA: $\|u\| = 0.016$, $\|v\| = 0.053$	Fig. 4
0.2	−0.07	SF	ODA to ES	OZP II	ODA go until time = 40	Fig. 2
0.22	−0.157	SF	ODA to ES	OZP II	ODA go until time = 20	Fig. 2
0.25	−0.26	SF	ODA to ES	OZP II	ODA go until time = 12	Fig. 2
0.3	−0.54	SF	ODA to ES	OZP II	ODA go until time = 8	Fig. 2
0.5	−0.63	SN	ES	No	No oscillation	No

All other parameters corresponding to OZP II are fixed. Starting point is close to the unique equilibrium state (ES): $u = 0.29$, $v = 1.43$. Designations: σ, trace of Jacobian matrix of linearized dynamic model (Eq. (1)); UF, unstable focus; CE, center; SF, stable focus; SN, stable node; OIA, oscillations with increasing amplitude; OCA, oscillations with constant amplitude; LC, limit cycle; ODA, oscillations with decreasing amplitude; ALC, amplitude of limit cycle; AOCA, amplitude of oscillations with constant amplitude.

Table 3. Changes in Character of Zoning and Type of Equilibrium State Using Different Values of θ

θ	σ	Type of ES 1	Pattern development	Type of OZP	Quantitative characteristics	Figure for comparison
0.1	1.93	UF	OIA to ES 2	OZP III	OIA go until time = 2	Fig. 3
0.2	0.47	UF	OIA to ES 2	OZP III	OIA go until time = 7	Fig. 3
0.25	0.17	UF	OIA to ES 2	OZP III	OIA go until time = 23	Fig. 3
0.27	0.09	UF	OIA to ES 2	OZP III	OIA go until time = 46	Fig. 3
0.2934	0	CE	OCA	OZP IV	AOCA: $\|u\| = 0.027$, $\|v\| = 0.01$	Fig. 4
0.3	−0.02	SF	ODA to ES 1	OZP II	ODA go any time	Fig. 2
0.35	−0.16	SF	ODA to ES 1	OZP II	ODA go until time = 25	Fig. 2
0.4	−0.27	SF	ODA to ES 1	OZP II	ODA go until time = 20	Fig. 2
0.5	−0.41	SF	ODA to ES 1	OZP II	ODA go until time = 10	Fig. 2
0.6	−0.51	SN	ES1	No	No oscillations	No

All other parameters corresponding to OZP III are fixed. Starting point is closed to the equilibrium state (ES 1): $u = 0.39$, $v = 1.22$. Designations: σ, trace of Jacobian matrix of the linearized dynamic model (Eq. (1)); UF, unstable focus; CE, center; SF, stable focus; OIA, oscillations with increasing amplitude; OCA, oscillations with constant amplitude; ODA, oscillations with decreasing amplitude; AOCA, amplitude of oscillations with constant amplitude.

(SF) after a region of ODA, similar to that shown in Figure 2. The appearance of ODA corresponds to values of θ from 0.3 to 0.5. The point at which the visible oscillations disappear occurs earlier as θ becomes bigger. When θ is 0.6 and higher, the model (Eq. (1)) does not produce oscillatory zoning.

EFFECT OF CONCENTRATIONS

For a given natural system, the parameter θ, the ratio of diffusivities of Ca^{2+} and H_2CO_3, is expected to be more or less fixed, but the actual concentrations of these two species may vary greatly. Here is an analysis of the behavior of the model (Eq. (1)) depending on the parameter γ, which is the product of θ and the ratio of concentrations of Ca^{2+} and H_2CO_3 far away from the crystal surface. Wang and Merino (1992) predicted the range for γ, such as $\gamma > 1.4$, where calcite can incorporate oscillatory concentrations for trace elements. Table 4 collects the results of our investigation of the behavior of the model (Eq. (1)) with changes in the value of γ between 1.7 and 6.0; all another parameters correspond to OZP III (Table 1) and are fixed. The initial conditions are chosen close to the equilibrium solution, which coordinates are different at different values of γ. In regard to the physical conditions, higher values of γ will correspond to the bulk concentration for Ca^{2+} increasing and or the bulk concentration for H_2CO_3 decreasing.

When γ is equal to 1.7, the model (Eq. (1)) has one equilibrium solution, a stable node (SN) with no oscillations. When γ is equal to 1.8, the model has also one equilibrium solution, a stable focus (SF), and behavior of the model is similar to that shown in Figure 2. When γ is equal to 1.85, two more equilibrium solutions appear: a saddle and an unstable focus (UF). A saddle does not produce oscillatory behavior. Behavior of the model near an unstable focus (ES2) is similar to that shown in Figure 3. As γ increases, the quantitative characteristics of pattern development near one equilibrium state (ES 1) are not changed, but those near another one (ES 2) are changed strongly: the time taken for OIA to change to ES 1 increases. When γ is equal to 2.137, the type of ES 2 changes to a center with the amplitude of oscillations, such as $|u| = 0.0023$, $|v| = 0.012$, similar to that shown in Figure 4. Further increases in γ results in the equilibrium state (ES 1) becoming a stable node, which disappears at $\gamma = 2.3$, and another second equilibrium state (ES 2) becoming a stable focus (SF) after a region of ODA similar to Figure 2. The appearance of ODA corresponds to values of γ from 2.2 to 5. The point at which the visible oscillations disappear occurs earlier as γ becomes bigger. When γ is 6 and higher, the model (Eq. (1)) does not produce oscillatory zoning.

APPLICATION TO A NATURAL OZP

Figure 5 shows a cathodolumenescence (CL) imaging of oscillatory zoning pattern in calcite crystal from the Rossland area, BC, Canada. This pattern was

Table 4. Changes in Character of Zoning and Type of Equilibrium State Using Different Values of γ

γ	σ	Type of ES 1	Pattern development	Quantitative characteristics	Figure for comparison	σ	Type of ES 2	Pattern development	Quantitative characteristics	Figure for comparison
1.7	−2.6	SN	ES 1	No oscillations	No					
1.8	−2.4	SF	ODA to ES1	ODA go until time = 1	Fig. 2					
1.85	−2.3	SF	ODA to ES1	ODA go until time = 1	Fig. 2	0.49	UF	OIA to ES 1	OIA go until time = 10	Fig. 3
1.95	−2.0	SF	ODA to ES1	ODA go until time = 1	Fig. 2	0.25	UF	OIA to ES 1	OIA go until time = 20	Fig. 3
2.0	−1.9	SF	ODA to ES1	ODA go until time = 1	Fig. 2	0.17	UF	OIA to ES 1	OIA go until time = 25	Fig. 3
2.1	−1.6	SF	ODA to ES1	ODA go until time = 1	Fig. 2	0.04	UF	OIA to ES 1	OIA go until time = 86	Fig. 3
2.137	−1.4	SF	ODA to ES1	ODA go until time = 1	Fig. 2	0	CE	OCA	AOCA: $\lvert u\rvert = 0.0023$, $\lvert v\rvert = 0.012$	Fig. 4
2.2	−1.0	SN	ES 1	No oscillations	No	−0.06	SF	ODA to ES 2	ODA go any time	Fig. 2
2.3						−0.15	SF	ODA to ES 2	ODA go until time = 20	Fig. 2
3.2						−0.57	SF	ODA to ES 2	ODA go until time = 5	Fig. 2
4.0						−0.72	SF	ODA to ES 2	ODA go until time = 1	Fig. 2
6.0						−0.87	SN	ES 2	No oscillations	No

All other parameters corresponding to OZP III are fixed. Starting points are closed to the equilibrium states, and they are different for different values of γ. Designations: σ, trace of Jacobian matrix of the linearized dynamic model (Eq. (1)); UF, unstable focus; CE, center; SF, stable focus; OIA, oscillations with increasing amplitude; OCA, oscillations with constant amplitude; ODA, oscillations with decreasing amplitude; AOCA, amplitude of oscillations with constant amplitude.

studied by Bryksina and Halden (2005) by analyzing laser ablation microprobe data for trace elements: Mn, Fe and Sr. Using statistical and fractal characteristics it was described as a sequence of quantitatively different patterns: Part 1, . . . , Part 6 (Fig. 5).

In this paper, we describe this natural pattern qualitatively using the four general OZPs produced by the model (Eq. (1)). Natural oscillatory zoning patterns in calcite can appear very complicated, than we see in the model simulations. However, some qualitative features of the modeled OZPs are consistent with the natural example. Part1 and Part 6 show no zones (Fig. 5). Part2 shows weak oscillatory zoning, has small changes in intensity of color similar to OZP IV, and is labeled as type IV. Of the next three parts showing distinct oscillatory character, Part 3 has four sub-zones, two of them show small variations of light color changing to small variations of dark color; these are also labeled as type IV. We might suggest that the dynamics of calcite growth in this case had two non-saddle equilibrium solutions including a center, and the pattern development was from unstable equilibrium state to stable one. Another sub-zone of Part 3 is marked as type III because it shows increasing color intensity changing to homogenous color similar to OZP III. The last sub-zone of Part 3 has decreasing intensity of color similar to OZP II, this is labeled as type II. By analogy, Part 4 has three sub-zones; the first one is similar to OZP III and last two to OZP II. All three sub-zones of Part 5 show an asymmetric gradational change in color similar to OZP I, these are labeled as I. So, using the four modeled OZPs, the natural oscillatory zoning pattern can be described as a sequence of eleven growth stages.

DISCUSSION AND CONCLUSIONS

This paper describes four qualitatively different types (OZP I, OZP II, OZP III, OZP IV) of behavior of the self-organizational dynamic model proposed by Wang and Merino (1992) and displays them as simulated cathodoluminescence

Figure 5. CL image of oscillatory zoning pattern in calcite crystal from the Rossland area, British Columbia, Canada. The numbers 1, 2, 3, 4, 5, 6 are the designations for quantitatively different parts 1, . . . , 6 of the pattern respectively (Bryksina and Halden, 2005). The labels I, II, III, IV are the designations for OZP I, OZP II, OZP III, OZP IV respectively. The scale rule is equal to 1 mm.

images. In terms of these OZPs, the behavior of the model was investigated depending on the parameter θ, which is the ratio of diffusivities of Ca^{2+} and H_2CO_3. It was shown that small changes in values of θ may produce qualitatively similar OZP with different quantitative characteristics, and big changes in values of θ may produce qualitatively and quantitatively different OZPs. The special case of bifurcation parameter values is also shown, when small changing in values of θ may produce qualitatively different OZPs. Because the parameter θ plays special role in the model (the number and the coordinates of the equilibrium solutions do not depend of θ), two examples of the influence of θ on the model were described (Tables 2 and 3). By changing this parameter we see how the numerically identical equilibrium solution changes in type and or between stable and unstable states.

The behavior of the model was also investigated depending on the parameter γ (Table 4), which is the product of θ and the ratio of concentrations of Ca^{2+} and H_2CO_3 far away from the crystal surface. It was shown that small changes as well as big changes in values of γ may produce not only quantitatively different OZPs, but also qualitatively different OZPs, because this parameter influences the number of equilibrium solutions and their disposition in phase space. The results of the investigation of the behavior of the model depending on the other parameters, such as λ, β_1 and β_1, show that the influence of these parameters on the model is similar to that described for parameter γ.

This paper also shows that the dynamics proposed by Wang and Merino (1992) can be used as a reasonable analogue for Mn distribution in natural calcite. An oscillatory zoning pattern in calcite crystal from the Rossland area (BC, Canada) is described in terms of four general OZPs produced by the model (Eq. (1)). According to previous study (Bryksina and Halden, 2005), along the chosen profile, this natural OPZ can be presented as a sequence of six quantitatively different parts, which represent the response of the crystal to some external geological event that brought the system sufficiently far from equilibrium, such as the influx of new fluid or a sudden temperature change. As it follows from the cathodoluminescence image of the natural pattern (Fig. 5), there are no zones at the beginning (Part 1) and at the end (Part 6) of the crystal. All other parts show one, two or three different modeled patterns, which would be a result of its own growth dynamics: Part 2 shows OZP IV; Part 3 shows OZP IV, OZP III, OZP IV and OZP II; Part 4 shows OZP III, OZP II and OZP II; Part 5 shows OZP I, OZP I and OZP I. So, in one crystal we can see how the pattern evolves as a sequence of OZPs. The cathodoluminescence image of synthetic OZP shown by Reeder, Fagioli, and Meyers (1990, Fig. 2a) is similar and it can be described by the model proposed by Wang and Merino (1992) and qualitatively characterized as OZP II.

As a consequence of the modeling we see that different OZPs have different dimensionless times (time) for one cycle of the oscillatory zoning. The fastest

process corresponds to OZP I (time=2), then goes OZP II (time=3), then OZP III (time=8.5), and the slowest process corresponds to OZP IV (time=45). Therefore, we suggest that the rate of crystal growth changes during the formation of oscillatory zoning in this crystal. Using *very fast*, *fast*, *slow* and *very slow* to describe the rate of growth of parts 2 to 5, the OZP would indicate a growth history that followed this sequence: *very slow, very slow, slow, very slow, fast, slow, fast, fast, very fast, very fast, very fast*. So, the modeled OZPs have allowed us not only to describe qualitatively the natural OZP, but also to compare crystal growth rates in different parts of the crystal. In the natural setting the next step will be to compare the growth histories of adjacent crystals and crystals from different environments.

ACKNOWLEDGMENTS

This work was done with the assistance of an NSERC Discovery Grant to NMH and an NSERC-NATO PDF to NAB.

REFERENCES

Allegre, C. J., Provost, A., and Jaupart, C., 1981, Oscillatory zoning: A pathological case of crystal growth: Nature, v. 294, p. 223–228.

Andronov, A. A., Leontovich, E. A., Gordon, I. I., and Maier, A. G., 1967, The theory of bifurcations of dynamic systems on a plane: Nauka, Moscow, 496 p.

Bryxina, N. A., and Sheplev, V. S., 1997, Oscillatory zoning in calcite growing from an aqueous solution: Math. Model., v. 9, no. 6, p. 33–38.

Bryxina, N. A., Dublyansky, Yu. V., Halden, N. M., Campbell, J. L., and Teesdale, W. J., 2000a, Statistical characteristics of oscillatory zoning in cave calcite - popcorn from Hungary: Dokl. Akad. Nauk., v. 372, no. 4, p. 514–517.

Bryxina, N. A., Sheplev, V. S., Ripinen, O. I., Halden, N. M., Campbell, J. L., and Teesdale, W. J., 2000b, Oscillatory zoning in agate: qualitative analyses of the Wang-Merino dynamic model and quantitative estimates of trace elements distributions in a specimen from Arts-Bogdo (Mongolia): Russian Geol. Geophys., v. 41, no. 9, p. 1243–1254.

Bryxina, N. A., Halden, N. M., Ripinen, O. I., and Reverdatto, V. V., 2001a, Trace elements in agate from Khazahstan (the environs of city Pavlodar): Dokl. Akad. Nauk, v. 376, no. 4, p. 519–522.

Bryxina, N. A., Sheplev, V. S., 2001b, Algorithm of calculation of Lyapounov Coefficients for analysis of chemical autooscillations, as applied to calcite crystallization model: Math. Geol., v. 33, no. 8, p. 993–1010.

Bryxina, N. A., Halden, N. M., and Ripinen, O. I., 2002, Oscillatory zoning in an agate from Kazakhstan: autocorrelation functions and fractal statistics of trace element distributions: Math. Geol., v. 34, no. 8, p. 915–927.

Bryksina, N. A., and Halden, N. M., 2005, Oscillatory zoning in calcite from the Rossland area, British Columbia, Canada: statistical and fractal characteristics of trace element distributions, *in* Cheng, Q., and Bonham-Carter, G., eds., GIS and Spatial Analysis, Proceedings of IAMG'05, York University, Toronto, v. 1, p. 323–328.

Fowler, A. D., and L'Heureux, I., 1996, Self-organized banded sphalerite and branching galena in the Pine Point ore deposit, Northwest Territories: Can. Mineral., v. 34, p. 1211–1222.

Haase, C. S., Chadam, J., Feinn, D., and Ortoleva, P., 1980, Oscillatory zoning in plagioclase feldspar: Science, v. 209, p. 272–274.

Halden, N. M., 1996, Determination of Lyapounov exponents to characterize the oscillatory distribution of trace elements in minerals: Can. Mineral., v. 34, p. 1127–1135.

Holten, T., Jamtveit, B., and Meakin, P., 2000, Noise and oscillatory zoning of minerals: Geochim. Cosmochim. Acta, v. 64, p. 1893–1904.

Jamtveit, B., 1991, Oscillatory zonation patterns in hydrothermal grossular-andradite garnet: Nonlinear dynamics in regions of immiscibility: Am. Mineral., v. 76, p. 1319–1327.

Jamtveit, B., Wogelius, R. A., and Fraser, D. G., 1993, Zonation patterns of scarn garnets: Records of hydrothermal system evolution: Geology, v. 21, p. 113–116.

Katsev, S., and L'Heureux, I., 2000, Impact of environmental noise on oscillatory pattern formation in crystal growth: Plagioclase feldspar: Phys. Rev. E, v. 61, p. 4972–4949.

L'Heureux, I., and Fowler, A. D., 1996, Isothermal constitutive undercooling as a model for oscillatory zoning in plagioclase: Can. Mineral., v. 34, p. 1137–1147.

L'Heureux, I., and Jamtveit, B., 2002, A model of oscillatory zoning in solid solutions grown from aqueous solutions: Applications to the $(Ba,Sr)SO_4$ system: Geochim. Cosmochim. Acta, v. 66, no. 3, p. 417–429.

Li, Y.-H., and Gregory, S., 1974, Diffusion of ions in sea water and in deep-sea sediments: Geochim. Cosmochim. Acta, v. 38, no. 5, p. 703–714.

Merino, E., 1984, Survey of geochemical self-patterning phenomena, *in* Nicolis, G., and Baras, F., eds., Chemical Instabilities, D. Reidel, Dordrecht, p. 305–328.

Merino, E., and Wang, Y., 2001, Self-organization in rocks: Occurences, observations, modeling, testing – With emphasis on agate genesis, *in* Krug, H. J., and Ktuhl, J. H., eds., Non-equilibrium Processes and Dissipative Structures in Geosciences, Self-Organization Yearbook. Duncker & Humblot, Berlin, v. 11, p. 13–45.

Nicolis, G., and Prigogine, I., 1977, Self-organization in non-equilibrium system: John Wiley & Sons, New York, 491 p.

Ortoleva, P., Merino, E., Moore, C., and Chadam, J., 1987, Geochemical self-organization, I: Reaction-transport feedbacks and modeling approach: Am. J. Sci., v. 287, p. 979–1007.

Pearce, T. H., and Kolisnik, A. M., 1990, Observations of plagioclase zoning using interference imaging: Earth Sci. Rev., v. 29, p. 9–26.

Reeder, R. J., Fagioli, R. O., and Meyers, W. J., 1990, Oscillatory zoning of Mn in solution-grown calcite crystals: Earth Sci. Rev., v. 29, p. 39–46.

Shore, M., and Fowler, A. D., 1996, Oscillatory zoning in minerals: A common phenomenon: Can. Mineral., v. 34, p. 1111–1126.

Wang, Y., and Merono, E., 1990, Self-organizational origin of agates: banding, fiber twisting, composition and dynamic crystallization model: Geochim. Cosmochim. Acta, v. 54, p. 1627–1638.

Wang, Y., and Merino, E., 1992, Dynamic model of oscillatory zoning of trace elements in calcite: Double layer, inhibition, and self-organization: Geochim. Cosmochim. Acta, v. 56, p. 587–596.

Wang, Y., and Merino, E., 1993, Oscillatory magma crystallization by feedback between the concentrations of the reactant species and mineral growth rates: J Petrol., v. 34, p. 369–382.

Wang, Y., and Merino, E., 1995, Origin of fibrosity and banding in agates from flood basalts: Am. J. Sci., v. 295, p. 49–77.

Wang, J. H., and Wu, J. P., 1995, Oscillatory zoning of minerals and self-organization in silicate solid-solution systems: A new nonlinear dynamic model: Eur. J. Mineral., v. 7, p. 1089–1100.

Yardley, B. W. D., Rochelle, C. A., Barnicoat, A. C., and Lloyd, G. E., 1991, Oscillatory zoning in metamorphic minerals: an indicator of infiltration metasomatism: Mineral. Mag., v. 55, p. 357–365.